

The 2011 M_w 9.0 Tohoku Earthquake: Comparison of GPS and Strong-Motion Data

by Rongjiang Wang, Stefano Parolai, Maorong Ge, Mingpei Jin,
Thomas R. Walter, and Jochen Zschau

Abstract Near-field ground-motion data are available in semi-real time either from modern strong-motion or continuous Global Positioning System (GPS) networks, allowing robust solutions for earthquake source parameters, which are useful for rapid disaster assessment and early warning. These wide applications require the ground-motion data to cover a very broad frequency band that, however, is usually not available. This paper presents a case study on the 2011 M_w 9.0 Tohoku earthquake, showing how the ground-motion information from geodetic and seismic instruments is complementary, and suggesting the joint use of both types of data, particularly when the network coverage is sparse. First the strong-motion records from the two Japanese networks, K-NET and KiK-Net, are analyzed using an automatic empirical baseline correction tool. The static coseismic displacement data are obtained by double integration and then used to derive the permanent slip distribution on the earthquake fault. Comparisons with the corresponding GPS-based solutions yield a quantitative estimation of uncertainties of the empirical baseline correction. Furthermore, a dozen nearby GPS and strong-motion station pairs are selected to demonstrate that the information in their time series agrees with each other. Finally, methods for combining both types of ground-motion observation systems are discussed, and the wide applicability of this approach is highlighted.

Introduction

Transient and permanent ground movements caused by earthquakes are crucial for locating their source and for investigating their rupture processes. The transient and dynamic movements are usually measured by seismic sensors deployed worldwide, resulting in velocity or acceleration seismograms, while permanent displacements are traditionally measured through geodetic methods.

On the one hand, the continuous and rapid development of Global Positioning System (GPS) hardware and the improvement in GPS data processing strategies have been such that estimating seismic displacements from high-rate GPS has become a research topic referred to as GPS seismology (e.g., Larson *et al.*, 2003; Bock and Prawirodirdjo, 2004; Chen *et al.*, 2004; Langbein and Bock, 2004; Miyazaki *et al.*, 2004; Elósegui *et al.*, 2006; Larson, 2009; Irwan *et al.*, 2011). Currently, GPS seismology focuses on the acquisition of high-rate GPS data and the refinement of data processing approaches (Smalley, 2009). On the other hand, recent studies have shown that large near-source static displacements can also be derived from high-quality accelerometer records after an empirical baseline correction (e.g., Graizer, 1979, 1983; Iwan *et al.*, 1985; Boore, 2001; Wang, Boore, *et al.*, 2003; Wu and Wu, 2007; Chao *et al.*, 2009; Wang *et al.*, 2011).

Therefore, the joint use of the GPS and strong-motion instruments can improve data coverage and can advance the development of new strategies for data processing due to their complementary advantages (Emore *et al.*, 2007; Bock *et al.*, 2012). However, a systematic test and comparison of such data streams as well as their joint influence on kinematic source models has not yet been made.

Japan has one of the densest GPS and seismometer networks in the world, and presently includes the GeoNet, with 1200 permanent GPS stations, the F-Net, with 84 broadband seismograph stations, the K-NET, with 1000 strong-motion seismograph stations, the Hi-Net, with 777 high sensitivity seismograph stations (borehole installation), and the KiK-Net, co-located with the Hi-Net. Each KiK-Net station is equipped with two strong-motion seismographs at the surface and borehole, respectively (see [Data and Resources](#)). Additional data, such as InSAR, were also collected, though not further considered in this study. Nevertheless, after the 2011 M_w 9.0 Tohoku earthquake, an unprecedented amount of ground-motion data were available from these observation networks, providing an ideal opportunity for evaluating the consistency of the ground motion obtained by the different observation instruments.

In this study, we first focus on assessing the uncertainties of the estimated displacement values, starting from strong-motion data, and investigate their effect on the earthquake source inversion results. In particular, we present a new approach to detect outliers in the derived dataset. This allows us to evaluate whether a joint inversion of the two datasets represents a valid option when networks are sparser than in Japan. We also examine the validity of our results for data coverage much sparser than in the present case. Finally, we compare the displacement and velocity seismograms derived from the high-rate GPS and the strong-motion records and show how they are complementary over a broad frequency band.

Comparison between Static Coseismic Displacements Derived from the Strong-Motion and GPS Recordings

In order to obtain reliable estimates of permanent displacement, we first analyze the complete strong-motion dataset collected by both K-NET and KiK-net using the automatic empirical baseline correction scheme proposed by Wang *et al.* (2011). The empirical baseline correction method is based on the same concept first proposed by Iwan *et al.* (1985), in which a bilinear function is used to describe the velocity trend induced by baseline errors in strong-motion records. Currently, several manual or automatic versions of the method have been described (see Wang *et al.*, 2011 and references therein). The only difference between them is the choice of the two timing parameters of the bilinear correction. In the method by Wang *et al.* (2011), the timing parameters are determined in a way so that the corrected displacement history best fits a step function. After the baseline correction, velocity and displacement seismograms are obtained through integration over time. The permanent displacement, also commonly called coseismic displacement, is then estimated from the postevent plateau of the corrected displacement history. Although the latter might be underrepresented in this routine, the strong-motion data may provide important information on the initial deformation as described below.

Figure 1 shows a site map of the GeoNet, K-NET, and KiK-Net stations in the area of investigation. Coseismic displacements are derived from K-NET, KiK-Net-SF (surface sensors), and KiK-Net-BH (borehole sensors), respectively, and are shown in Figure 2, where the high-precision GPS solutions are depicted as reference. In general, the KiK-Net-BH dataset leads to the most stable displacement values (with coherent spatial variability) that are also the closest to the GPS observations. The displacement vectors show a centralized direction to the earthquake source centroid as described below. The maximum displacement in the order of about 5 m was observed in the coast near Sendai by both GPS and KiK-Net stations. The K-NET dataset shows a large spatial variability in the displacements, also between stations that are close to one another. In fact, as the K-NET was designed

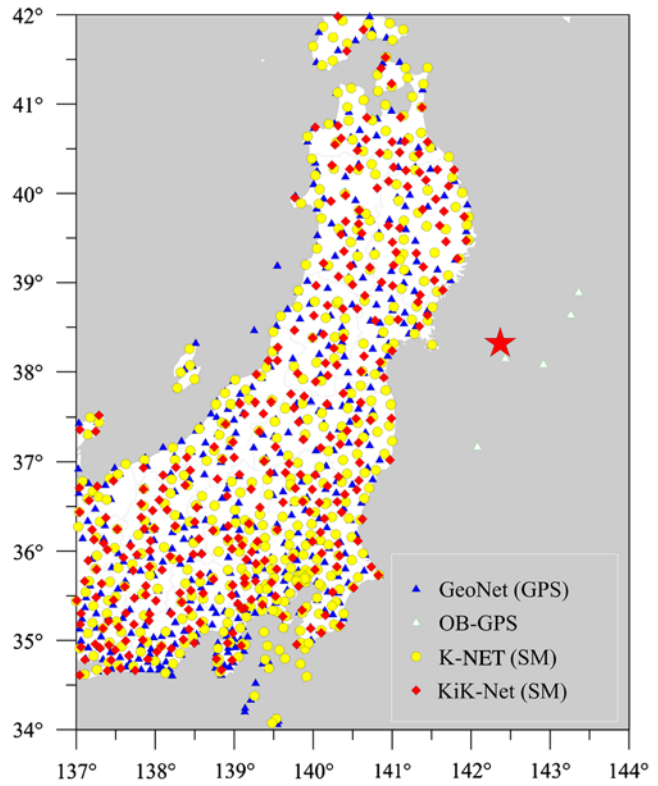


Figure 1. GPS and strong-motion (SM) stations of the GeoNet, the Ocean-Bottom GPS/Acoustic Network, the K-NET, and the KiK-Net, respectively, from which the data for the 2011 Tohoku earthquake used in this study originate. The star is the epicenter of the 2011 Tohoku earthquake (38.322° N, 142.369° E) as determined by the USGS. The color version of this figure is available only in the electronic edition.

mainly for rapid response purposes, most stations are located in public offices, schools, parks and on free-surface of softer sediments than those of KiK-Net (Tsuda *et al.*, 2006; Aoi *et al.*, 2011). Possibly, the amplified response of the soft soil below these stations led to large transient tilting of the accelerometers (Graizer 2005, 2010). For this reason, coseismic displacements derived from the K-NET data will not be further discussed. Some isolated anomalous displacement values that are not coherent with those obtained by nearby stations are also observed for a few KiK-Net surface sensors. An example of such an anomaly is shown by the surface sensor at the KiK-Net station FKSH18 (37.4894° N, 140.5380° E), which even shows an east–west displacement not consistent with the retrieved general trend (Fig. 3). We conjecture this kind of anomaly to be mainly due to the nonlinear baseline shift affecting the strong-motion recordings, which cannot be properly accounted for using the bilinear correction scheme (Fig. 3). Theoretically, the ground tilt does not affect the vertical component so strongly. This is verified in the present case. No extreme anomalous values appear in the vertical displacement derived from both K-NET and KiK-Net datasets.

Before comparing the source models in the following section, we compare the coseismic displacements derived

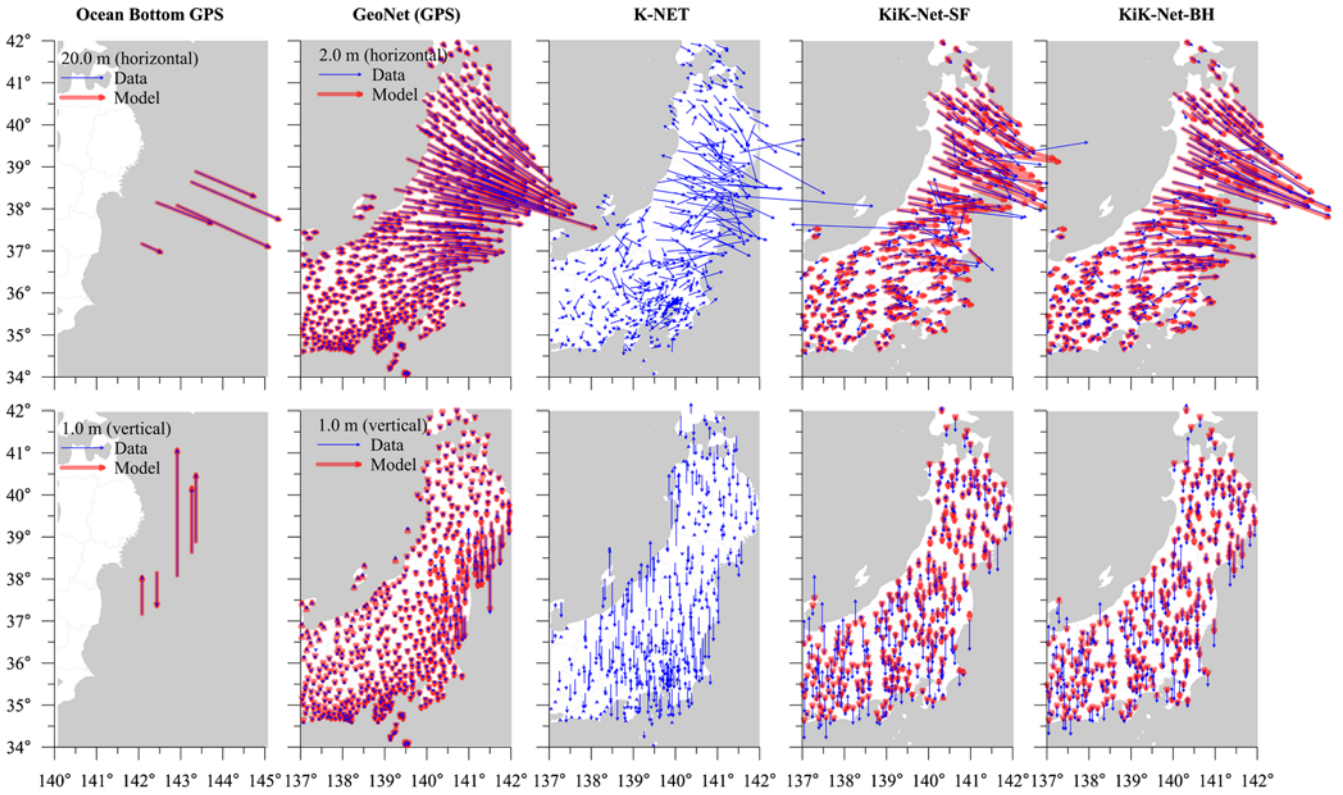


Figure 2. Coseismic displacement data derived from different GPS and strong-motion networks for the 2011 Tohoku earthquake, compared with the values predicted by Models 1–3 (Fig. 4) inverted from the respective dataset. No model is derived from the K-NET dataset because of its large uncertainty. The model for both the onshore and offshore GPS datasets is obtained by joint inversion. The color version of this figure is available only in the electronic edition.

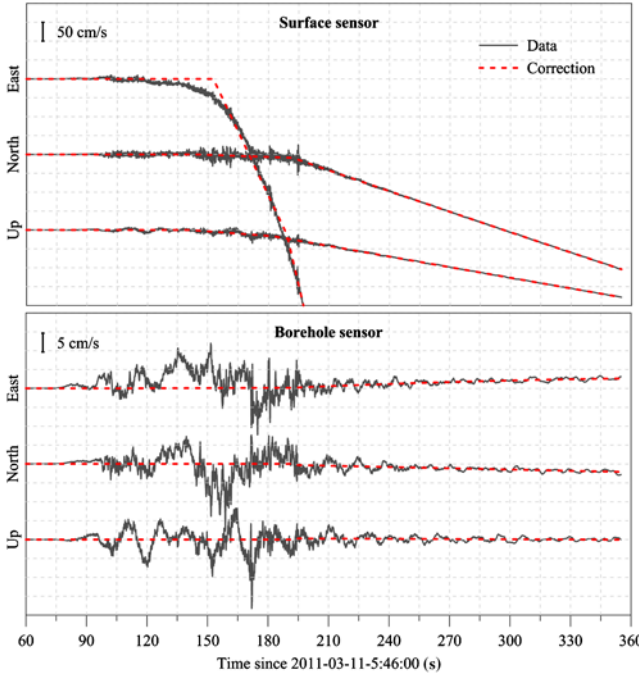


Figure 3. Ground velocity derived from the records of both surface and borehole accelerometers at KiK-Net station FKSH18 (37.4894° N, 140.5380° E). The baseline corrections are estimated using the automatic scheme by Wang *et al.* (2011). The color version of this figure is available only in the electronic edition.

from the KiK-Net-BH data with those interpolated from the GPS. The root mean square (rms) of the deviatoric displacement vectors between the two datasets is 0.47 m, or 37% of the rms of the absolute KiK-Net-BH displacement vectors, which is 1.25 m. Therefore, given the large coseismic displacement associated with the M_w 9.0 Tohoku earthquake, those two datasets compare well and provide independent observation points, which may have an effect on the source models as shown below.

Comparison between Source Models Derived from the GPS and Strong-Motion Derived Coseismic Displacement Data

In order to assess the effect of the largest uncertainties in the coseismic displacement data derived by strong-motion recordings on the earthquake source modeling, we invert the static slip distribution from the two KiK-Net datasets separately, and we compare the obtained results with those obtained by the high-precision GPS data.

The inversions are carried out using a self-developed software (FORTRAN code “SDM” by R. Wang) based on the constrained least-squares method, which has been used in a number of recent studies on geodetic slip models (Motagh *et al.*, 2008, 2010; Wang *et al.*, 2009, 2011; Diao *et al.*, 2010, 2011; Xu *et al.*, 2010). For simplicity of numerical

analysis, the fault plane is represented by a number of small rectangular dislocation patches with uniform slip. The observed displacement data are related to the discrete fault slips through Green's functions of the earth model, which are calculated using linear elastic dislocation theory. For the discrete slips to be an adequate representation of the true continuous slip distribution, the patch size must be reasonably small (Segall and Harris, 1987). In fact, if the available data do not include enough information for determining the slip distribution with the desired resolution, the inversion system becomes underdetermined. To overcome the problem of non-uniqueness and instability inherent in such an underdetermined system, *a priori* conditions (fixed fault geometry and restricted variation range for the rake angle) and physical constraints (smooth spatial distribution of slip or stress drop) are considered (Du *et al.*, 1998).

In the present case, we employ a slightly curved fault plane, parallel to the assumed subduction slab. The dip angle increases linearly from 10° on the top (ocean bottom) to 20° at about 80 km depth, which is consistent with that suggested by Pollitz *et al.* (2011). To avoid any artificial bounding effect, a large enough potential rupture area (approximately 650 km \times 300 km) is used. The upper edge of the fault is located along the trench east of Japan, on the boundary between the Pacific plate and the Eurasian plate. The patch size is about 10 km \times 10 km. The rake angle determining the slip direction at each fault patch is allowed to vary between $90^\circ \pm 20^\circ$, corresponding to the upper bound of the uncertainties of the teleseismic focal solutions. Green's functions are calculated based on a multilayered elastic half-space model (Wang, Lorenzo-Martin, Roth, 2003; Wang *et al.*, 2006). The model parameters are chosen according to the database CRUST2.0 (Bassin *et al.*, 2000). The weighting factor for the smoothing term, also called the smoothing factor, is optimized first for the inversion of the complete GPS data including the offshore observations adopted from Sato *et al.* (2011), and then is fixed for all other inversions.

The inversion results are shown in Figure 4. Because of the high station density of all considered networks, we assume that differences in the results are related to the different quality of the input data for the inversion. The best resolved slip model is assumed to be that derived from the high-precision GPS data, including both onshore and offshore observations. In fact, this model indicates that the peak coseismic slip of the earthquake reached about 50 m which is in agreement with previous results obtained by the joint inversion of onshore GPS and deep ocean tsunami data by Simons *et al.* (2011), but larger than the peak slip of 33 m obtained by Pollitz *et al.* (2011) who also used both the onshore and offshore GPS data but a slightly different fault geometry (three connected rectangles) and approximated the slip distribution by analytical Hermite-Gauss functions. Other recently published slip models that are only based on the onshore GPS data show peak slips systematically below 35 m (e.g., Iinuma *et al.*, 2011; Ozawa *et al.*, 2011), whereas those only based on teleseismic waveform data show large

scatters between 30 and 60 m (e.g., Ammon *et al.*, 2011; Lay *et al.*, 2011). The moment magnitude of the earthquake is estimated to be 8.90, in agreement with that given by the global seismic network GEOFON. It should be noted that when calculating the seismic moment, we adopted the commonly used constant shear modulus $\mu_o = 30$ GPa instead of using the depth dependent shear modulus given by the earth model. If the latter is used, the geodetic moment magnitude would reach 9.01. The reason for using the constant shear modulus is that here we want to compare the different slip models in terms of slip magnitude instead of the associated seismic moment. Hence, the shear modulus used here only plays the role of a scaling factor.

Using the best geodetic slip model as a reference, Model 3 (see Fig. 4) derived from the KiK-Net-BH dataset is very satisfactory and considerably better than that from the KiK-Net-SF dataset (Model 2, Fig. 4), which strongly underestimates the magnitude of the earthquake. It is interesting that peak slip values as large as 50 m can only be obtained when seafloor GPS data are used. Without this data, the GPS-derived slip model (Model 4) is very close to that from the KiK-Net-BH dataset (Model 3), with both showing similar patterns where the peak slip is less than 25 m. The datafit of Model 3 to the onshore GPS data is equally as good as the datafit of Model 1.

A Model-Based Approach for Detecting Outliers in the Strong-Motion Derived Coseismic Displacements

In the previous two sections we have shown, consistent with previous studies elsewhere, that the large coseismic displacements during the Japan 2011 Tohoku earthquake can also be retrieved reliably from strong-motion records using an empirical baseline correction tool. Although the displacement values obtained at a few individual stations may include large uncertainties, a robust source solution can still be derived when the whole dense network is considered, provided that the sensors are installed in boreholes or at least on hard ground. In practice, such ideal installation conditions are not always fulfilled, not only due to financial or logistic limitations, but also because many strong-motion stations were installed intentionally on soft sediments and urban areas for engineering purposes. Therefore, large baseline errors may be induced by the amplified and transient tilt effect, and in general they cannot fully be corrected using the empirical bilinear correction method. Consequently, obvious outliers appear in the strong-motion derived displacement data (see Fig. 2). Because these outliers may affect the results of the slip inversion, we propose a model-based approach to detect them.

First we invert, for example, the total KiK-Net-SF dataset to obtain a preliminary slip model. A certain observed surface displacement in the input dataset is defined as an outlier if its misfit to the predicted one oversteps a certain threshold. As an example, Figure 5 shows the two KiK-Net datasets after having removed the outlier vectors, which deviate from the model by more than 15° in direction. Here the 15° threshold in direction is chosen so that the filtered

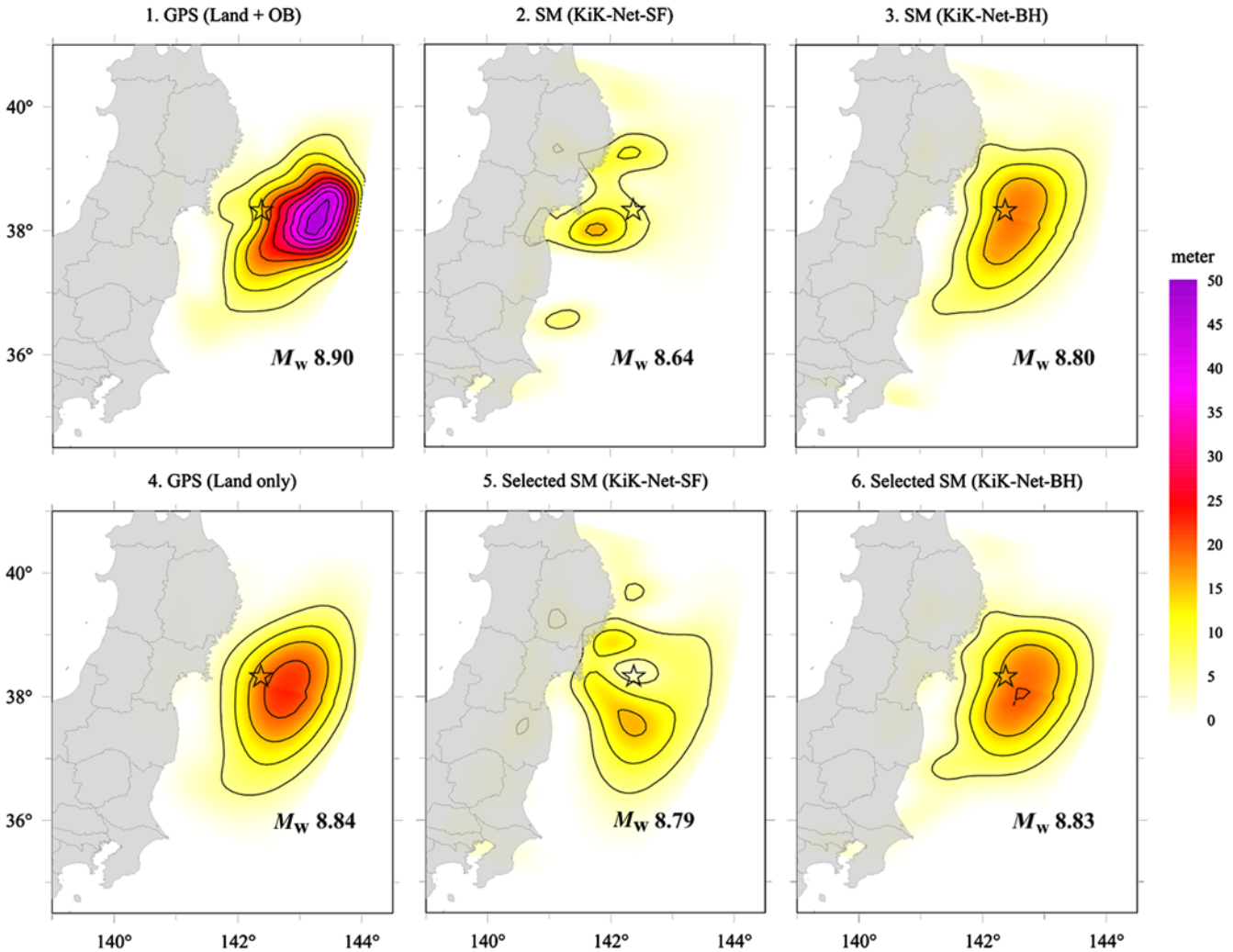


Figure 4. Slip models inverted from different coseismic displacement datasets (OB, ocean bottom; SM, strong motion derived; SF, surface sensor; and BH, borehole sensor). The data are shown in Figure 2. The selected KiK-Net surface and borehole data are shown in Figure 5. Both horizontal and vertical components are used for the inversion. The contour step is 5 m. The color version of this figure is available only in the electronic edition.

KiK-Net-SF data can still show a reasonable coherence of their spatial variability. We do not filter the outlier displacements on the basis of the vector amplitude because it has less influence on constraining the source location. After filtering the outliers, the statistical deviation of the KiK-Net-BH dataset from the GPS is reduced from 37% to 20% in the present case.

In areas with a high station density, the outliers can also be easily detected by comparison between neighboring stations, but the model-based detection method also works for inhomogeneous networks. It is worth noting that, when using the filtered data, we can improve the slip model considerably, particularly with respect to the moment magnitude in the case of the KiK-Net-SF dataset (Model 5 in Fig. 4). Because of their relatively small amplitudes, most of the vertical components are within the uncertainty range of the method.

In most other regions of the world, both geodetic and seismic networks are generally sparser than in Japan. Because we

have shown that the strong-motion data derived displacement has an acceptable quality when compared with that directly measured by GPS, the combination of the individual observation systems could improve the data coverage in those regions and thus reduce the uncertainties of earthquake source inversion when only based on GPS data. To simulate such a situation, we make a test in which 25 displacement vectors are randomly selected from the GPS and KiK-Net-SF datasets (without the outliers), respectively. As shown in Figure 6, although only about 10% of the original data are used, the earthquake source can be resolved satisfactorily. We attribute the result to the remaining azimuth coverage of the data and the improved data quality after filtering the outliers.

Comparison between Time Series of GPS and Strong-Motion Records

Another important utility of high-rate GPS and strong-motion networks is to provide near-field seismic waveform

data, which are useful for constraining the kinematic earthquake source process. In practice, the low-frequency band of waveform information is particularly useful for inversion of

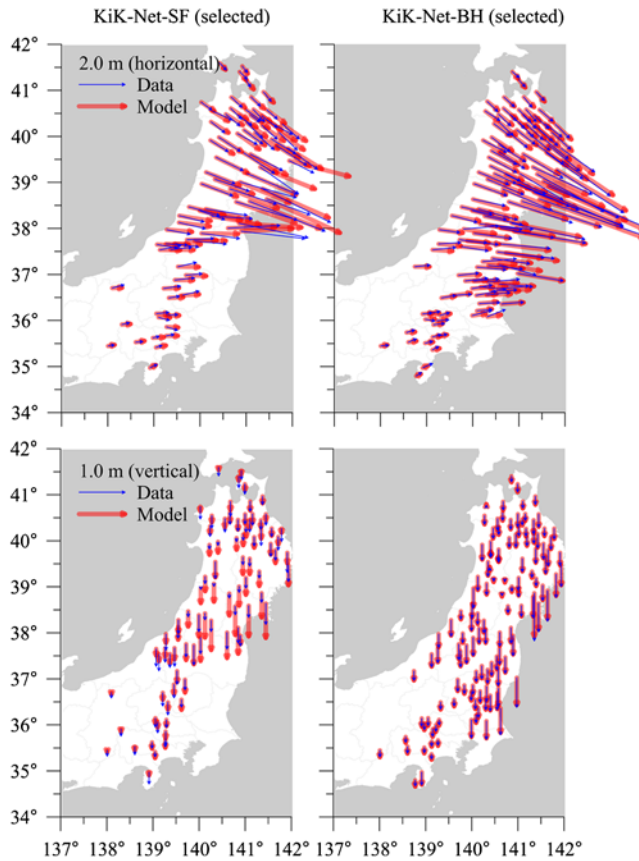


Figure 5. Coseismic displacement data derived from strong-motion records at selected KiK-Net stations, where the observed 3D displacement vector deviates from that predicted by Models 2 and 3 in Figure 4, respectively, by less than 15° in direction. The color version of this figure is available only in the electronic edition.

source time function. Thus, we need to derive velocity or displacement seismograms from strong-motion records, for which the empirical baseline correction is also necessary. Without the baseline correction, certain high-pass or band-pass filters have to be applied to the strong-motion records, leading to loss of the information about low-frequency as well as static ground deformation that is important for estimating the moment magnitude.

The uncertainties of the strong-motion derived velocity or displacement seismograms can be best evaluated using co-installed high-rate GPS as reference. Although Japan has the densest GPS and strong-motion networks in the world, there are rare stations where both types of instruments are co-installed. Nevertheless, we found more than a dozen collocated (or nearly collocated) GeoNet and KiK-Net station pairs. Using the automatic baseline correction scheme by Wang *et al.* (2011), we derive the velocity and displacement seismograms from the strong-motion recordings and compare them with the GPS data for all 14 station pairs with distance ≤ 4 km (Fig. 7). In only a few cases the strong-motion derived displacement seismograms show significant deviations from the high-rate GPS data, mostly in the period after the permanent displacement has arrived. The worst results are obtained for the borehole sensor of KiK-Net station FKSH07 (No. 14 in Fig. 7), where the derived east–west displacement converges to an opposite final value with respect to the GPS. This is partly due to the fact that in this case, the strong-motion records do not allow us to select enough pre-event and post-event times, which are necessary for a successful empirical baseline correction using the automatic scheme. In all other cases, however, the velocity seismograms derived from the high-rate GPS and strong-motion records agree satisfactorily with each other, supporting previous observations that the uncertainties of the empirical baseline correction can affect the derived velocity seismograms, but not as dramatically as for the displacement seismograms (Boore, 2001).

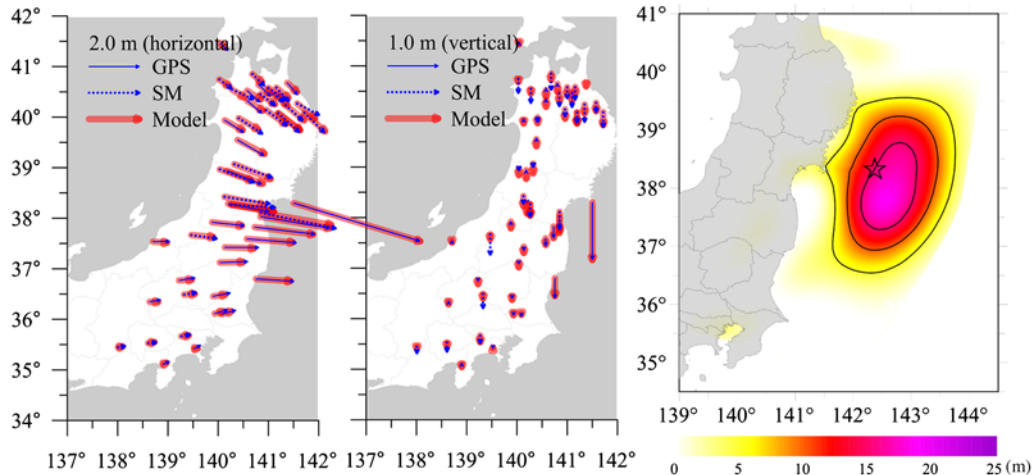


Figure 6. Coseismic displacement data randomly selected from the GPS and KiK-Net-SF datasets (Fig. 2) and the associated slip model by joint inversion. The color version of this figure is available only in the electronic edition.

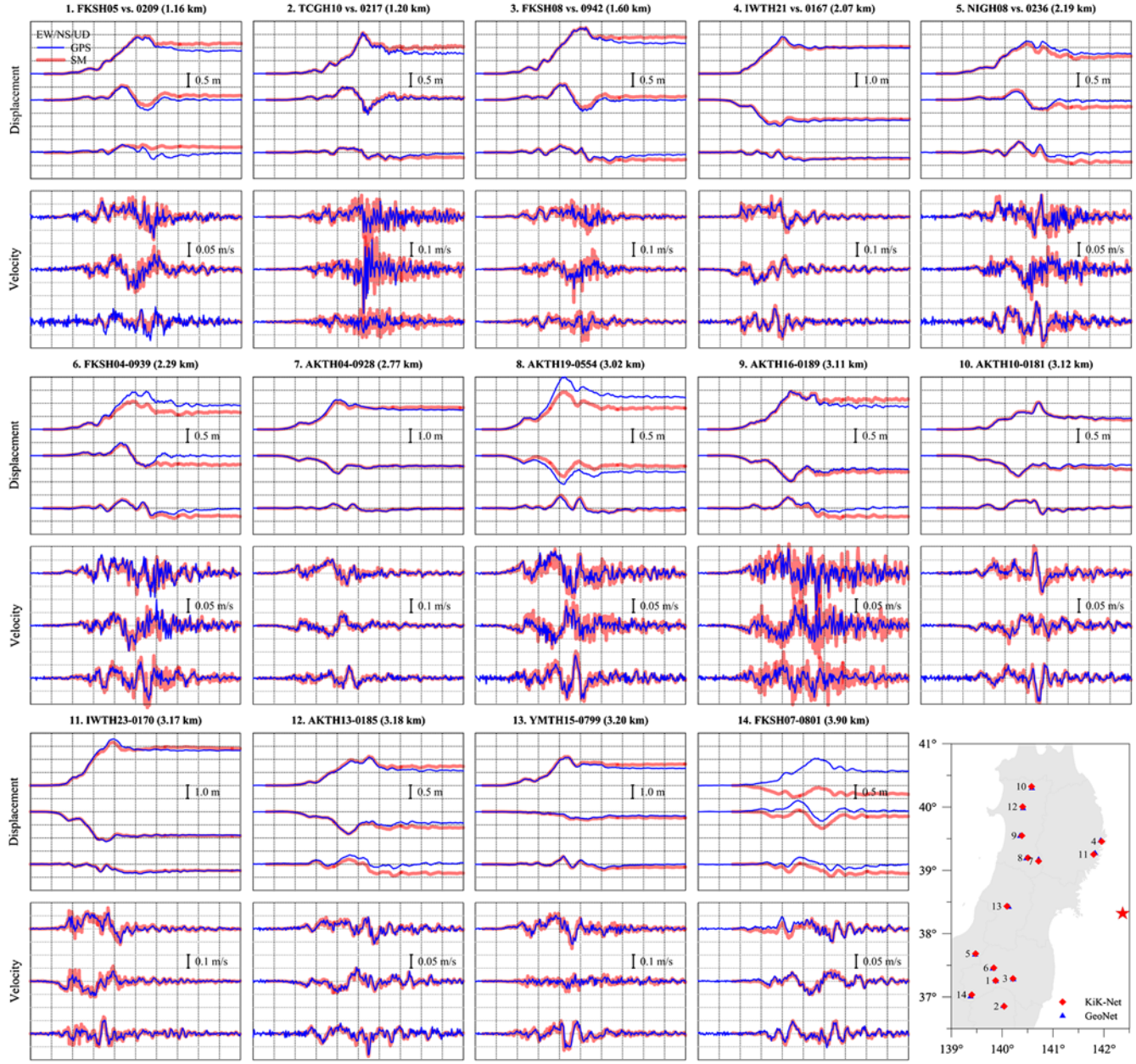


Figure 7. Displacement and velocity seismograms of the 2011 Tohoku earthquake derived from the KiK-Net borehole strong-motion records using the automatic baseline correction tool by Wang *et al.* (2011), compared with nearby GPS observations. The number for each station pair corresponds to the number in the station map. The time window is uniformly 250 s. The color version of this figure is available only in the electronic edition.

Joint Use of High-Rate GPS and Strong-Motion Records

In previous studies dealing with other major earthquakes, such as the 1999 Chi-Chi (Taiwan), 2007 Tocopilla (Chile), and 2008 Wenchuan (China) earthquakes (Wu and Wu, 2007; Wang *et al.*, 2011), the high-rate GPS data from permanent stations were not available, but the static coseismic displacement of the strong-motion stations was well estimated from temporary GPS networks or InSAR observations. Therefore, it is interesting to investigate whether the

empirical baseline correction can be improved upon using the known coseismic displacement as reference. We suggest a modification of the criterion for choosing the timing parameters so that the final displacement is closest to the GPS reference. Our results show that the use of the GPS reference can obviously improve the recovery of the displacement history from the strong-motion records (Fig. 8), providing more accurate low-frequency waveform data that are useful for investigating the rupture process of the earthquake.

For nearly co-installed GPS and strong-motion stations, the true ground-motion information at a broad frequency

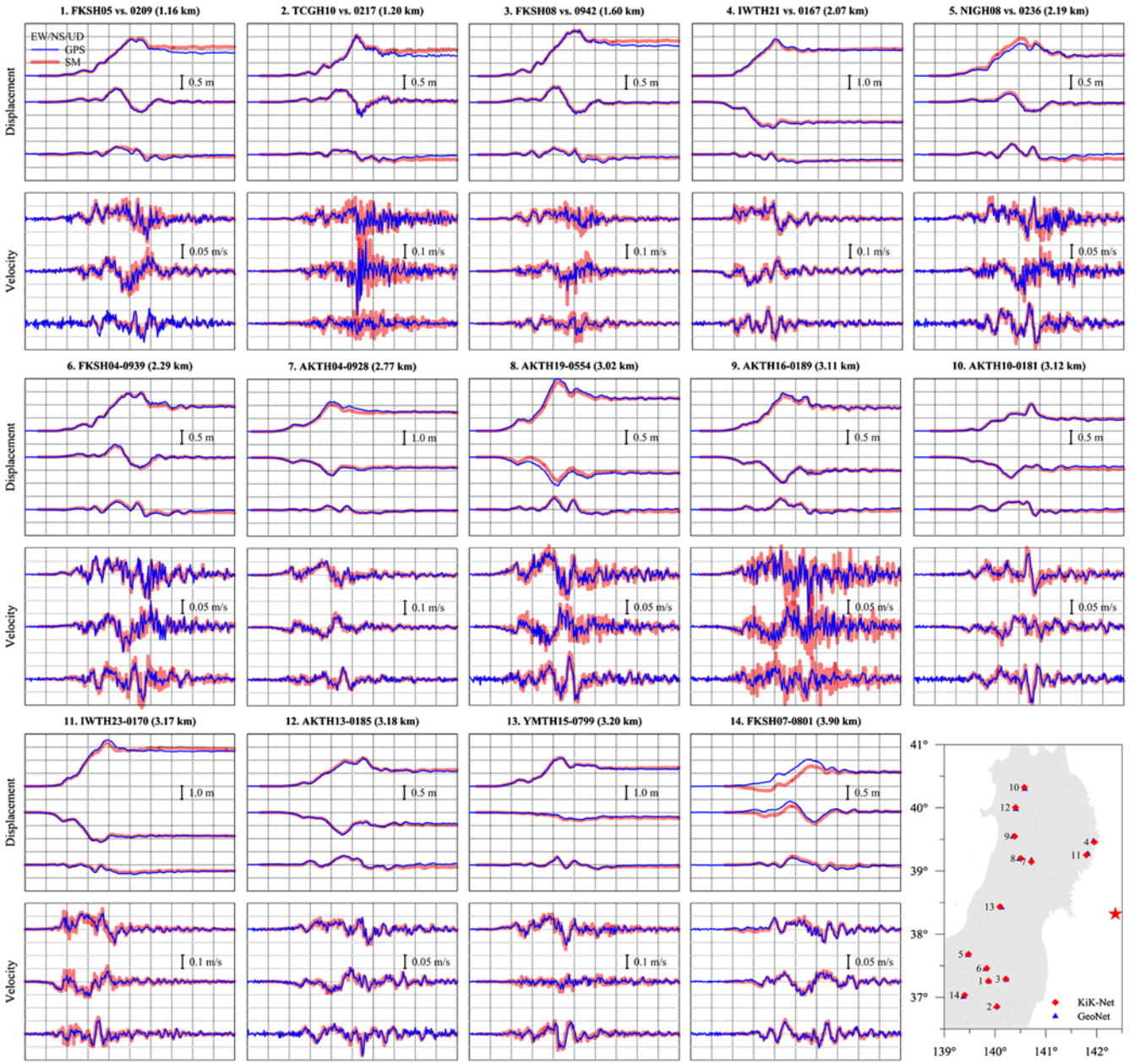


Figure 8. Same as Figure 7, but the permanent GPS displacement is used as a reference in the baseline correction of strong-motion records. The color version of this figure is available only in the electronic edition.

band can be retrieved by the joint use of the two instruments. As an example, we select the nearest station pair between the strong-motion and GPS networks, that is, K-NET station AKT006 (40.2152° N, 140.7873° E) and the GeoNet station 0183 (40.2154° N, 140.7873° E), being separated by 20 m. Figure 9 shows clearly the problems of both observation techniques. The ground tilting leads to large erroneous trends in the two horizontal displacement components obtained by double integration of the strong-motion records, whereas the ground acceleration is strongly underestimated by the double derivatives of the GPS displacement. Because of the low sampling rate (1 Hz) of GPS, high-frequency content is missing and possible aliasing effects might appear after double dif-

ferentiations. In the following we propose a simple approach for the utility of joint GPS and strong-motion records.

We first remove the pre-event offset from the GPS data. Then we assume that the baseline error of each component of the accelerometer is time dependent and can be expressed generally by a linear function combined with a sinusoidal series,

$$B(t) = a + bt + \sum_{n=1}^N c_n \sin\left(2n\pi \frac{t}{T}\right), \quad t \in [0, T],$$

where $[0, T]$ is the time window of the data, and a , b , and c_n ($n = 1, 2, \dots, N$) are free parameters to be determined.

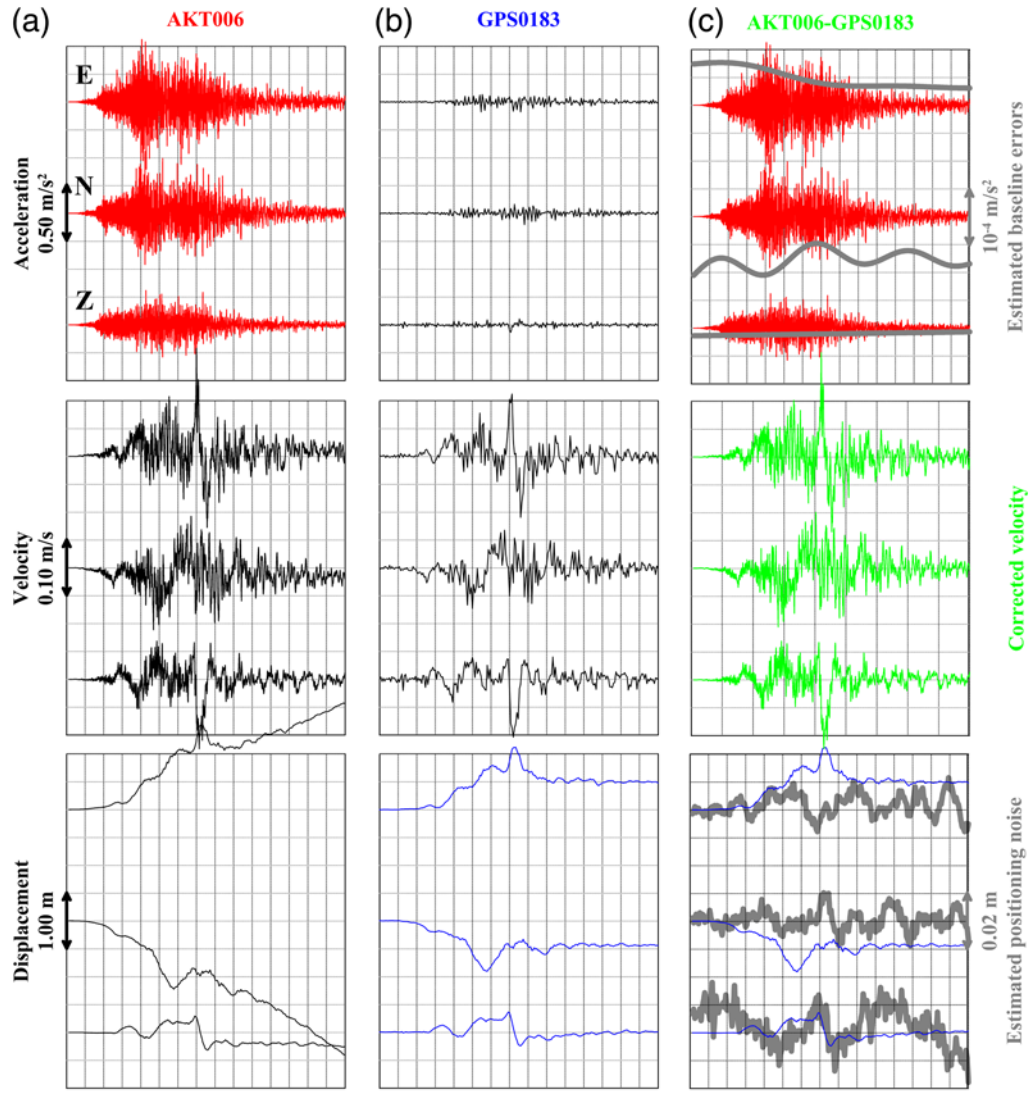


Figure 9. (a) The 100 Hz strong-motion records (top) at K-NET Station AKT006, the velocity (middle) and displacement seismograms (bottom) integrated from the strong-motion records, respectively. (b) The acceleration (top) and velocity seismograms (middle) differentiated from the 1 Hz GPS time series (bottom) measured at GeoNet Station 0183, respectively. (c) The acceleration (top), velocity (middle) and displacement seismograms (bottom) obtained using joint use of the strong-motion and GPS data. The thick gray curves in the right-top and right-bottom panels are the estimated strong-motion baseline errors and GPS positioning errors, respectively. The time window is uniformly 225 s. The color version of this figure is available only in the electronic edition.

The linear term represents the permanent as well as the slow trend of the baseline, whereas the sinusoidal series, which starts and ends with zero, covers the transient baseline errors during the strong shaking period. Because the two stations are nearly co-located, their seismic movements should be almost the same for the great Tohoku earthquake that nucleated at about 250 km distance. Thus, we propose to determine the free parameters in a way where the displacement obtained by double integration of the strong-motion recordings, after removing the baseline errors, best fits the GPS data in a least-squares sense. The number of the free parameters for the baseline correction depends on the required fitting error of the strong-motion derived displacement to the GPS data.

In principle, the larger the degree N , the better the strong-motion derived displacement fits the GPS data. On the other hand, N should be as small as possible to avoid any overweighting of the GPS in the joint processing because the GPS is known to have larger high-frequency noise. Generally we start with $N = 0$ and then, if necessary, increase it until the required fitting is satisfied or a certain upper limit of N is arrived. The results shown in Figure 9 are obtained by requiring the fitting error not larger than ± 1 cm for the two horizontal components and ± 2 cm for the vertical component, corresponding roughly to the measurement errors of the GPS. It turns out that $N = 5, 8$, and 0 for the east, north, and vertical components, respectively. Though the functions

used for the baseline correction (thick gray curves in the right-top panel, Fig. 9c) are very smooth, the misfits between the strong-motion based displacements and the GPS data (thick gray curves in the right-bottom panel, Fig. 9c) are likely uncorrelated with the high-frequency seismic signals. Therefore, these misfits might be attributed to stochastic observation noises in both strong-motion data and GPS data, but also to some effects caused by different installation conditions between the two instruments. Figure 9 also shows the ground velocity (right-middle panel) recovered by the joint use of the GPS and strong-motion data, which provides a basis for the broadband ground-motion data. On this basis, one can obtain the ground displacement (right-bottom panel) by integration and the ground acceleration (right-top panel) by differentiation, both with a resolution that is much higher than is derived from the geodetic and seismic observations separately.

Discussion and Conclusions

Japan has the densest geodetic and seismic networks in the world. In the case of major earthquakes, information about ground motion is available near real time through these networks. Using an automatic empirical baseline correction scheme, we analyzed the accelerograms recorded by the K-NET and KiK-Net strong-motion networks for the 2011 Tohoku earthquake. The coseismic displacements derived from the KiK-Net borehole dataset are the closest to the high-precision GPS solutions. In comparison, the KiK-Net surface dataset shows larger uncertainties, but still appears to be robust when the whole network is considered. Less confident results for the derived coseismic displacements are those from the K-NET dataset showing large spatial variability. Probably the strongly amplified soil response including surface tilting (Bonilla *et al.*, 2011) caused complicated and multiple baseline shifts for most of the K-NET sensors, as well as for some of the KiK-Net surface sensors, leading to the failure of the simple bilinear correction scheme.

We inverted the static slip distribution from the two KiK-Net datasets, respectively, and compared it with that obtained from the high-precision GPS data. When the commonly used constant shear modulus $\mu_o = 30$ GPa is adopted to convert the slip to the seismic moment, the moment magnitude of the earthquake derived from either the strong-motion based or GPS coseismic displacement field is about 8.8 to 8.9, slightly less than the final CMT solution of 9.0 by the U.S. Geological Survey (USGS), but consistent with the GEOFON value. Currently, most slip models derived by the inversion of near-field geodetic data are based on a uniform elastic half-space mainly because it allows us to calculate Green's functions in a closed analytical form. It is known that the static displacement due to a dislocation source in a uniform elastic half-space is dependent upon the Poisson ratio, but independent of the absolute value of the shear modulus of the medium. This might not be valid for the layered structure; neglecting this issue may lead to errors of up

to 20% in the static surface displacement (Pollitz, 1996). Moreover, recent studies have shown that when the inversion is made based on models incorporating depth-dependent shear moduli, the derived seismic moment can be up to 40% greater because of deeper source location than that based on the uniform half-space model (Hearn and Bürgmann, 2005). In order to determine the moment magnitude independently, the effect of the layered crustal structure should be accounted for when inverting the geodetic data. We note that a more complex fault geometry may have an effect on the interpretation of the data.

After an empirical correction for the baseline errors, the ground velocity and displacement histories are derived from the strong-motion records through the integration over time. Generally, the slip model results obtained from inverting the KiK-Net data agree considerably better with those derived from the high-rate GPS observations than those from the K-NET data. The latter appear to be strongly affected by site effects (strong nonlinear trends in the recordings that could be due to large and transient tilting of the sensor installed on soft ground) and thus cannot be used until an efficient procedure for correcting them is found. The velocity time histories derived from the KiK-Net borehole records are barely influenced by the residual uncertainties still existing after the empirical baseline correction and are more informative, because of the higher sampling rate (100 Hz), than the 1-Hz GPS data for the ground-motion characterization in terms of velocity and therefore energy.

It is desirable that the ground-motion data cover a frequency band as broad as possible so that they can be used for different geophysical and engineering investigations. In order to verify if this is the case when strong-motion and GPS data are considered, we made a comparison of the datasets in the acceleration, velocity, and displacement domains, which dominate different frequency bands of the surface deformation information. On the one hand, we integrated the KiK-Net-BH strong-motion records after the empirical baseline correction to obtain velocity and displacement seismograms. On the other, we differentiated the high-rate GPS time series to receive the velocity seismograms, but did not derive the acceleration seismograms, since the low 1-Hz sampling rate of the GPS data would only allow a comparison with a low-pass filtered version of the accelerogram. Although theoretically the highest sampling rate of GPS receivers nowadays may reach 50 Hz, it is expected that the derived acceleration would be very noisy and could not, with any real confidence, be used as an alternative to the strong-motion recordings.

We also attempted to evaluate, and verify, whether the baseline correction of the strong-motion records proposed by Wang *et al.* (2011) can be improved upon when using the GPS coseismic displacement as reference. The results we obtained are successful in terms of comparability of the velocity and displacement histories estimated from the GPS and strong-motion data, respectively. Furthermore, we demonstrated an example in which both high-rate GPS and strong-motion data from a co-located site are combined to

recover the ground-motion information over a broad frequency band (0–100 Hz). It is expected that there will be increasingly co-installed high-rate GPS and strong-motion networks and the joint GPS and strong-motion data processing will become useful for real-time inversion of the kinematic source process and therefore of great impact for earthquake and tsunami early warning.

Data and Resources

The K-NET and KiK-Net strong-motion data for the 2011 Tohoku earthquake were provided by the National Research Institute for Earth Science and Disaster Prevention (NIED) of Japan and are available from <http://www.k-net.bosai.go.jp/> and <http://www.kik.bosai.go.jp/> (last accessed June 2011), respectively. All original GeoNet GPS data were provided by the Geospatial Information Authority (GSI). The GPS coseismic displacement data produced by the ARIA team at JPL and Caltech were downloaded from <ftp://sideshow.jpl.nasa.gov/pub/usrs/ARIA/> (last accessed March 2011). The 1-Hz GPS data (of the GSI via Nippon GPS Data Services Company [NGDS]) were downloaded from http://rtgps.com/rtnet_dl_eq.php (last accessed April 2011). The teleseismic focal solution of the 2011 Tohoku earthquake was adopted from <http://geofon.gfz-potsdam.de/data/alerts/2011/gfz2011ewla/mt.txt> (last accessed March 2011). The CRUST2.0 model was downloaded from <http://igppweb.ucsd.edu/~gabi/crust2.html> (last accessed March 2011).

Acknowledgments

We thank Walter Zürn and Adrien Oth for valuable discussion, and Kevin Fleming for proofreading of the manuscript. This work is partly supported by the Towards Real-Time Earthquake Risk Reduction (REAKT) project of the European Seventh Framework Programme (Grant Agreement Number 282862). Mingpei Jin is supported by the China Scholarship Council and China Earthquake Administration. The comments of two anonymous reviewers were very helpful for improving the quality and readability of the paper.

References

- Ammon, C. J., T. Lay, H. Kanamori, and M. Cleveland (2011). A rupture model of the 2011 off the Pacific coast of Tohoku Earthquake, *Earth Planets Space* **63**, 693–696.
- Aoi, S., T. Kunugi, H. Nakamura, and H. Fujiwara (2011). Deployment of new strong motion seismographs of K-NET and KiK-net, *Geotech. Geol. Earthq. Eng.* **14**, 167–186, doi: [10.1007/978-94-007-0152-6_12](https://doi.org/10.1007/978-94-007-0152-6_12).
- Bassin, C., G. Laske, and G. Masters (2000). The current limits of resolution for surface wave tomography in North America, *EOS Trans. AGU* **81**, F897.
- Bock, Y., and L. Prawirodirdjo (2004). Detection of arbitrarily large dynamic ground motions with a dense high-rate GPS network, *Geophys. Res. Lett.* **31**, L06604, doi: [10.1029/2003GL019150](https://doi.org/10.1029/2003GL019150).
- Bock, Y., D. Melgar, and B. W. Crowell (2012). Real-time strong-motion broadband displacements from collocated GPS and accelerometers, *Bull. Seismol. Soc. Am.* **101**, 2904–2925, doi: [10.1785/0120110007](https://doi.org/10.1785/0120110007).
- Bonilla, L. F., K. Tsuda, N. Pulido, J. Régnier, and A. Laurendeau (2011). Nonlinear site response evidence of K-NET and KiK-net records from the 2011 Tohoku earthquake, *Earth Planets Space* **63**, 1–7.
- Boore, D. M. (2001). Effect of baseline corrections on displacement and response spectra for several recordings of the 1999 Chi-Chi, Taiwan, earthquake, *Bull. Seismol. Soc. Am.* **91**, 1199–1211.
- Chao, W., Y. Wu, and L. Zhao (2009). An automatic scheme for baseline correction of strong-motion records in coseismic deformation determination, *J. Seismol.* **14**, 495–504.
- Chen, J., K. M. Larson, Y. Tan, K. W. Hudnut, and K. Choi (2004). Slip history of the 2003 San Simeon earthquake constrained by combining 1-Hz GPS, strong motion, and teleseismic data, *Geophys. Res. Lett.* **31**, L17608, doi: [10.1029/2004GL020448](https://doi.org/10.1029/2004GL020448).
- Diao, F., X. Xiong, and R. Wang (2011). Mechanism of transient post-seismic deformation following the 2001 M_w 7.8 Kunlun (China) earthquake, *Pure Appl. Geophys.* **168**, 767–779.
- Diao, F., X. Xiong, R. Wang, Y. Zheng, and H. Hsu (2010). Slip model of the 2008 M_w 7.9 Wenchuan (China) earthquake derived from the coseismic GPS data, *Earth Planets Space* **62**, 869–874.
- Du, Y., A. Aydin, and P. Segall (1998). Comparison of various inversion techniques as applied to the determination of a geophysical deformation model for the 1983 Borah Creek earthquake, *Bull. Seismol. Soc. Am.* **82**, 1840–1866.
- Elósegui, P., J. L. Davis, D. Oberlander, R. Baenaand, and G. Ekström (2006). Accuracy of high-rate GPS for seismology, *Geophys. Res. Lett.* **33**, L11308, doi: [10.1029/2006GL026065](https://doi.org/10.1029/2006GL026065).
- Emore, G. L., J. S. Haase, K. Choi, K. M. Larson, and A. Yamagiwa (2007). Recovering seismic displacements through combined use of 1 Hz GPS and strong-motion accelerometers, *Bull. Seismol. Soc. Am.* **97**, 357–378.
- Graizer, V. M. (1979). Determination of the true ground displacement by using strong motion records, *Izvestiya Acad. Sci. USSR, Phys. Solid Earth* (English edition) published by the American Geophysical Union and Geological Society of America, **15**, no. 12, 875–885.
- Graizer, V. M. (1983). The movement near the fault of the Gazli earthquake, *Izvestiya Acad. Sci. USSR, Phys. Solid Earth* (English edition) published by the American Geophysical Union and Geological Society of America, **19**, no. 3, 172–178.
- Graizer, V. M. (2005). Effect of tilt on strong motion data processing, *Soil Dynam. Earthq. Eng.* **25**, 197–204.
- Graizer, V. M. (2010). Strong motion recordings and residual displacements: What are we actually recording in strong motion seismology? *Seismol. Res. Lett.* **81**, 635–639.
- Hearn, E. H., and R. Bürgmann (2005). The effect of elastic layering on inversions of GPS data for coseismic slip and resulting stress changes: Strike-slip earthquakes, *Bull. Seismol. Soc. Am.* **95**, 1637–1653.
- Inuma, T., M. Ohzono, Y. Ohta, and S. Miura (2011). Coseismic slip distribution of the 2011 off the Pacific coast of Tohoku earthquake (M 9.0) estimated based on GPS data—Was the asperity in Miyagi-oki ruptured? *Earth Planets Space* **63**, 643–648.
- Irwan, M., F. Kimata, K. Hirahara, T. Sagiya, and A. Yamagiwa (2011). Measuring ground deformations with 1 Hz GPS data: The 2003 Tokachi-oki earthquake (preliminary report), *Earth Planets Space* **56**, 389–393.
- Iwan, W., M. Moser, and C. Peng (1985). Some observations on strong-motion earthquake measurement using a digital acceleration, *Bull. Seismol. Soc. Am.* **75**, 1225–1246.
- Langbein, J., and Y. Bock (2004). High-rate real-time GPS network at Parkfield: Utility for detecting fault slip and seismic displacements, *Geophys. Res. Lett.* **31**, L15S20, doi: [10.1029/2003GL019408](https://doi.org/10.1029/2003GL019408).
- Larson, K. M. (2009). GPS seismology, *J. Geod.* **83**, 227–233, doi: [10.1007/s00190-008-0233-x](https://doi.org/10.1007/s00190-008-0233-x).
- Larson, K. M., P. Bodin, and J. Gomberg (2003). Using 1 Hz GPS data to measure deformations caused by the Denali fault earthquake, *Science* **300**, 1421–1424.
- Lay, T., C. J. Ammon, H. Kanamori, L. Xue, and M. J. Kim (2011). Possible large near-trench slip during the great 2011 Tohoku (M_w 9.0) earthquake, *Earth Planets Space* **63**, 687–692.
- Miyazaki, S., K. M. Larson, K. Choi, K. Hikima, K. Koketsu, P. Bodin, J. Haase, G. Emore, and A. Yamagiwa (2004). Modeling the rupture

- process of the 2003 September 25 Tokachi-Oki (Hokkaido) earthquake using 1-Hz GPS data, *Geophys. Res. Lett.* **31**, L21603, doi: [10.1029/2004GL021457](https://doi.org/10.1029/2004GL021457).
- Motagh, M., B. Schurr, J. Anderssohn, B. Cailleau, T. R. Walter, R. Wang, and J.-P. Villotte (2010). Subduction earthquake deformation associated with 14 November 2007, M_w 7.8 Tocopilla earthquake in Chile; Results from InSAR and aftershocks, *Tectonophysics* **490**, 60–68.
- Motagh, M., R. Wang, T. R. Walter, R. Bürgmann, E. Fielding, J. Anderssohn, and J. Zschau (2008). Coseismic slip model of the August 2007 Pisco earthquake (Peru) as constrained by Wide Swath radar observations, *Geophys. J. Int.* **174**, 842–848.
- Ozawa, S., T. Nishimura, H. Suito, T. Kobayashi, M. Tobita, and T. Imakiire (2011). Coseismic and postseismic slip of the 2011 magnitude-9 Tohoku-Oki earthquake, *Nature* **475**, 373–376, doi: [10.1038/nature10227](https://doi.org/10.1038/nature10227).
- Pollitz, F. F. (1996). Coseismic deformation from earthquake faulting on a layered spherical earth, *Geophys. J. Int.* **125**, 1–14.
- Pollitz, F. F., R. Bürgmann, and P. Banerjee (2011). Geodetic slip model of the 2011 M 9.0 Tohoku earthquake, *Geophys. Res. Lett.* **38**, L00G08, doi: [10.1029/2011GL048632](https://doi.org/10.1029/2011GL048632).
- Sato, M., T. Ishikawa, N. Ujihara, S. Yoshida, M. Fujita, M. Mochizuki, and A. Asada (2011). Displacement above the hypocenter of the 2011 Tohoku-Oki earthquake, *Science* **332**, 1395.
- Segall, P., and R. Harris (1987). Earthquake deformation cycle on the San Andreas fault near Parkfield, California, *J. Geophys. Res.* **92**, 10,511–10,525.
- Simons, M., S. E. Minson, A. Sladen, F. Ortega, J. Jiang, S. E. Owen, L. Meng, J.-P. Ampuero, Sh. Wei, R. Chu, D. V. Helmberger, H. Kanamori, E. Hetland, A. W. Moore, and F. H. Webb (2011). The 2011 Magnitude 9.0 Tohoku-Oki earthquake: Mosaicking the mega-thrust from seconds to centuries, *Science* **331**, 1421–1425.
- Smalley, R. (2009). High-rate GPS: How high do we need to go? *Bull. Seismol. Soc. Am.* **99**, 1054–1061.
- Tsuda, K., J. Steidl, R. Archuleta, and D. Assimaki (2006). Site-response estimation for the 2003 Miyagi-Oki earthquake sequence considering nonlinear site response, *Bull. Seismol. Soc. Am.* **96**, 1474–1482.
- Wang, G., D. M. Boore, H. Igel, and X. Zhou (2003). Some observations on colocated and closely spaced strong ground-motion records of the 1999 Chi-Chi, Taiwan, earthquake, *Bull. Seismol. Soc. Am.* **93**, 674–693.
- Wang, L., R. Wang, F. Roth, B. Enescu, S. Hainzl, and S. Ergintav (2009). Afterslip and viscoelastic relaxation following the 1999 M 7.4 Izmit earthquake from GPS measurements, *Geophys. J. Int.* **178**, 1220–1237.
- Wang, R., F. Lorenzo-Martín, and F. Roth (2003). Computation of deformation induced by earthquakes in a multi-layered elastic crust—FORTRAN programs EDGRN/EDCMP, *Comput. Geosci.* **29**, 195–207.
- Wang, R., F. Lorenzo-Martín, and F. Roth (2006). PSGRN/PSCMP—A new code for calculating co- and post-seismic deformation, geoid and gravity changes based on the viscoelastic-gravitational dislocation theory, *Comput. Geosci.* **32**, 527–541.
- Wang, R., B. Schurr, C. Milkereit, Zh. Shao, and M. Jin (2011). An improved automatic scheme for empirical baseline correction of digital strong-motion records, *Bull. Seismol. Soc. Am.* **101**, 2029–2044.
- Wu, Y., and C. Wu (2007). Approximate recovery of coseismic deformation from Taiwan strong-motion records, *J. Seismol.* **11**, 159–170.
- Xu, C., Y. Liu, Y. Wen, and R. Wang (2010). Coseismic slip distribution of the 2008 M_w 7.9 Wenchuan earthquake from joint inversion of GPS and InSAR data, *Bull. Seismol. Soc. Am.* **100**, 2736–2749.

Helmholtz Centre Potsdam
GFZ German Research Centre for Geosciences
Telegrafenberg
14473 Potsdam, Germany
wang@gfz-potsdam.de
parolai@gfz-potsdam.de
maor@gfz-potsdam.de
twalter@gfz-potsdam.de
(R.W., S.P., M.G., T.R.W., J.Z.)

Western Yunnan Earthquake Prediction Test Site
China Earthquake Administration
1-1-301 Yuyuan Community
Wenhua Road, Dali 671000
People's Republic of China
jmp69@263.net
(M.J.)

Manuscript received 15 September 2012